EEET ECOLOGICAL ENGINEERING & ENVIRONMENTAL TECHNOLOGY

Ecological Engineering & Environmental Technology, 2026, 27(7), 419–435
https://doi.org/10.12912/27197050/224559
ISSN 2719–7050, License CC-BY 4.0

Received: 2026.05.06
Accepted: 2026.06.15
Published: 2026.07.01

Eco-efficient electric vehicle routing for municipal solid waste collection with payload-dependent energy consumption and carbon emissions

Hanane Ait Elasri[1*], Driss Khomsi[1], Naoual Semlali Aouragh Hassani[1]

[1] Hydraulic Systems Analysis Team (EASH), Civil Engineering Department, Mohammadia School of Engineers, Mohammed V University in Rabat, BP 765, Rabat, Morocco
* Corresponding author's e-mail: hanane_aitelasri@um5.ac.ma

ABSTRACT

The ecological management of municipal solid waste has become a strategic priority for sustainable urban development. Although many electric vehicle routing problem (EVRP) studies primarily focus on travel distance, the progressive variation of vehicle payload during collection operations can substantially affect electricity consumption and associated environmental impacts. This study aims to evaluate an eco-efficient EVRP framework that explicitly incorporates payload-dependent energy consumption and to investigate how payload sensitivity influences route evaluation and metaheuristic performance. The proposed model jointly considers travel distance, battery capacity, payload-sensitive energy consumption, and indirect CO_2 emissions. A comparative computational analysis was conducted using the Schneider benchmark dataset, where genetic algorithm (GA), particle swarm optimization (PSO), and simulated annealing (SA) were implemented under the same routing formulation and evaluated through a sensitivity analysis of the payload-sensitivity coefficient γ. The results demonstrate that incorporating payload-dependent energy consumption significantly changes the environmental assessment of routing solutions. The sensitivity analysis revealed a consistent distance–energy–emission trade-off. For GA, increasing γ from 0.00 to 0.10 reduced the average travelled distance from 1178.63 km to 1166.39 km, while energy consumption increased from 2180.47 to 2238.86 kWh and estimated emissions increased from 1565.58 to 1607.50 kg CO_2e. These findings indicate that shorter routes are not necessarily the most energy-efficient when payload effects are considered. GA exhibited the best overall performance across all scenarios, whereas PSO remained very competitive under moderate payload sensitivity and SA produced feasible but less competitive solutions. The study is limited to benchmark instances and a simplified payload-sensitive energy formulation. Nevertheless, the proposed framework provides a practical basis for integrating environmental considerations into electric waste collection planning. The originality of this work lies in explicitly quantifying how payload sensitivity affects energy consumption, CO_2 emissions, and algorithmic performance within a unified EVRP framework.

Keywords: electric vehicle routing problem, eco-efficient routing, metaheuristic algorithms, municipal solid waste collection, energy consumption.

INTRODUCTION

Municipal solid waste (MSW) management remains a major environmental challenge for sustainable urban planning, because currently collection operations generate high operational costs and environmental impacts. In many municipalities, MSW collection is one of the urban services most affected by the rapid urbanization and population growth, increasing pressure on municipal services and reinforcing the need for more efficient routing strategies. The use of electric vehicles (EVs) in MSW offers new opportunities to reduce the environmental footprint of urban services. However, EVs are not simply a direct replacement of conventional vehicles, they introduce additional operational restrictions related to limited battery capacity, energy consumption, and

the availability of charging infrastructure. These constraints can influence collection routes and therefore require specific optimization approaches that integrate energy and environmental criteria in route planning.

The electric vehicle routing problem (EVRP) belongs to the class of NP-hard problems, it extends the classical vehicle routing problem (VRP) by introducing specific constraints related to EVs, such as battery capacity and the dependence of travel costs on energy consumption. The optimization of the VRP has been investigated through several objectives, depending on the operational, economic, and environmental constraints. The most widely considered criteria include minimizing collection route length (Sarmah et al., 2019), reducing collection time (Carlos et al., 2019), managing waste content or collected waste quantities (Abdel-Shafy and Mansour, 2018), lowering operational costs (Rathore and Sarmah, 2019), and limiting environmental impacts (Ali et al., 2018). In order to improve operational realism, the optimization of EVRP is important because routing decisions are affected by real conditions of urban logistics, previous studies have also incorporated several practical constraints. Among these, vehicle capacity is one of the most common, since collection operations are directly limited by the payload capacity of waste collection trucks (Dotoli and Epicoco, 2017). Other constraints generally include service time restrictions, this is essential because in MSW collection, every collection point is not only a location to visit, but it requires also a service operation respecting a specific collection schedules (Bányai et al., 2019), characteristics of collection points or waste components (Yadav and Karmakar, 2020), environmental requirements (Pujara et al., 2019), regulatory conditions (Roberts et al., 2018), and other operational limitations.

Recent studies show that the EVRP is no longer treated only as a matter of minimizing distance, but also as a planning challenge involving operating costs, fuel use, emissions, service constraints, and urban variability. Multi-objective and dynamic formulations have therefore gained attention, particularly in works dealing with coordinated solid waste routing by integrating financial, environmental, and social objectives (Mojtahedi et al., 2021), multi-compartment and dynamic waste collection (Mohammadi et al., 2023), IoT-supported heuristic routing (Rahmanifar et al., 2023), and smart multi-compartment collection systems (Bouleft and Elhilali Alaoui, 2023). At the same time, GIS-based approaches and green routing models have shown their relevance in improving route design and environmental performance, as demonstrated by recent studies in geospatial route optimization (Das et al., 2024), green waste collection routing (Li et al., 2023), and capacitated waste collection using open-source optimization tools (Silva et al., 2023). Nevertheless, many existing approaches still prioritize distance, cost, or fuel consumption, while the effect of progressively accumulated payload on electricity use and CO_2 emissions remains less explicitly represented.

In addition, recent EVRP works have examined electric and hybrid waste collection vehicles under different operational settings, because waste collection is not a standard collection service problem, it involves heavy vehicles, changing payloads, frequent stops, and urban congestion. Therefore, hybrid vehicles are important because they reduce fuel use and emissions while offering more operational flexibility. In this context, Masmoudi introduced a plug-in hybrid electric refuse vehicle routing model with realistic energy functions (Amine Masmoudi et al., 2022), while Erdem examined heterogeneous EVs for sustainable recycling waste collection (Erdem, 2022). More recent contributions addressed EVRP for medical waste (Lin et al., 2024), classified waste collection with multi-compartment and multi-trip EVs (Liu et al., 2024), and MSW collection using EVs and variable neighborhood search (Zamanian et al., 2024). Other studies incorporated smart-bin information (Yang et al., 2022), charging station location-routing (Wang et al., 2022), energy differences among charging stations (Fan et al., 2023), collaborative multi-depot EVRP (Wang et al., 2023), and hybrid recharging with prioritized time windows (Zhang et al., 2024). These works confirm the relevance of EVRP for waste collection, but they also highlight a common limitation because many models require detailed traffic data, or real-time operational information, which can limit their reproducibility and transferability.

Despite this progress, a key research gap remains in the explicit modelling of payload-dependent energy consumption within EVRP formulations for MSW collection, where vehicle energy use should be treated as a function not only of travelled distance but also of the progressively accumulated payload along the route. In particular,

existing studies rarely quantify how the sensitivity of energy consumption to payload variation influences environmental indicators, route evaluation, and the relative performance of different metaheuristic optimization strategies.

The main objective of this study is to develop and evaluate an eco-efficient EVRP framework for MSW collection that incorporates payload-dependent energy consumption and investigates how variations in the payload-sensitivity coefficient γ affect travel distance, energy consumption, CO_2 emissions, and the comparative behavior of different metaheuristic algorithms. The study hypothesizes that increasing payload sensitivity alters the trade-off between distance minimization and energy efficiency, thereby changing the relative performance of three metaheuristics, namely genetic algorithm (GA), simulated annealing (SA), and particle swarm optimization (PSO), under identical routing conditions.

MATERIALS AND METHODS

Problem definition and eco-efficient formulation

The EVRP extends the classical VRP by incorporating both vehicle capacity and battery energy constraints, where a group of homogeneous EVs must collect waste from several geographically dispersed sites. Each EV begins and returns to a central depot and must respect maximum capacity and the energy efficiency of the vehicle battery, in the proposed model we adopt the following assumptions:

- All vehicles are identical in terms of payload capacity and battery capacity.
- Every collection point must be visited only by one vehicle.
- All routes start and end at the depot.
- Travel distances are computed based on benchmark coordinates using Euclidean geometry.
- Vehicles are homogeneous electric trucks.

We model the collection network as a graph $G= (V, A)$, where the parameters are defined in Table 1.

Table 1. Notation used in the EVRP formulation

$V= \{0, 1, ..., n\}$	Set of nodes; where 0 is the depot and 1 to n are the collection points
A	Set of arcs (i,j)
K	Group of EVs
k	Number of available vehicles
d_{ij}	Distance between node i and j
x_i, y_i	Cartesian coordinates of node i
q_i	Waste quantity at node i
Q	Vehicle capacity
B	Battery capacity
e_0	Baseline energy-consumption coefficient per unit distance
γ	Payload-sensitive energy coefficient
l_{ik}	Cumulative payload of vehicle k after serving node i
L_{ik}	Payload carried on arc (i,j)
E_{ijk}	Energy consumed by vehicle k travelling on arc (i,j)
EF	Factor of energy conversion to carbon

Decision variable

The main routing decision variable is: $x_{ijk} \in \{0,1\}$, it is equal to 1 if vehicle k travels from node i to j, or 0 otherwise for all $(i,j) \in V$.

Objective functions

To distinguish between the conventional routing perspective and the proposed eco-efficient formulation, two objective structures are considered in this study.

The baseline formulation minimizes only the total travel distance:

$$min\, f_1 = \sum_{k\epsilon K} \sum_{i\epsilon V} \sum_{j\epsilon V, j\neq i} d_{ij} x_{ijk} \qquad (1)$$

Distances between nodes were calculated using standard Euclidean metrics as presented follows:

$$d_{ij} = \sqrt{(x_i - x_j)^2 + (y_i - y_j)^2} \qquad (2)$$

This objective is essential because distance is a fundamental indicator in the operational sector, it corresponds to the conventional routing perspective in which route quality is evaluated under geometric compactness only.

From an environmental perspective, total fleet energy consumption is also considered as a relevant objective because it complements the distance objective by reflecting the operational reality of EVs:

$$\min f_2 = \sum_{k\epsilon K} E_k \qquad (3)$$

where: E_k is the total fleet energy consumption defined from the payload-sensitive energy model introduced below.

Payload-sensitive energy modelling

To reflect the fact that heavier collection vehicles require more energy, the study adopts a payload-sensitive energy formulation. In MSW collection, the vehicle leaves the depot with an empty payload and progressively accumulates waste along the route. In this study, the cumulative payload of vehicle k immediately after servicing node i is denoted by l_{ik} and the initial payload at the depot is:

$$l_{0k} = 0, \forall k \in K \tag{4}$$

If the vehicle k travels from node i to node j, the payload after servicing node j is updated as follows:

$$l_{jk} = l_{ik} + q_j, j \neq 0 \tag{5}$$

For the depot return, no additional waste is collected, so:

$$q_0 = 0 \tag{6}$$

The payload capacity condition is:

$$0 \leq l_{ik} \leq Q, \forall i \in V, \forall k \in K \tag{7}$$

The normalized payload ratio after servicing node i on arc (i,j) is:

$$L_{ijk} = l_{ik}/Q \; ; \; 0 \leq L_{ijk} \leq 1 \tag{8}$$

The energy consumed by vehicle k on arc (i,j) is defined as:

$$E_{ijk} = d_{ij} e_0 \left(1 + \gamma L_{ijk}\right) x_{ijk} \tag{9}$$

In the proposed energy model, we used e_0 =1.85 kWh/km as the reference electricity-consumption rate, following the mean distance-specific energy demand reported for electric waste collection vehicles under real-life operational data (Schmid et al., 2021).

The payload-sensitivity coefficient γ was introduced to represent the additional energy consumption associated with the progressively accumulation of waste payload during collection operation. Three values were tested: γ=0.00, γ=0.05, and γ=0.10. The selected values were chosen to represent three controlled payload-sensitivity scenarios. The first case γ=0.00 is used as a no-payload reference scenario, in this case energy consumption depends only on travelled distance. The values γ=0.05 and γ=0.10 represent moderate and stronger payload-sensitivity scenarios. This choice is justified because when the vehicle is fully loaded (L_{ijk} = 1), the values γ=0.05, and γ=0.10 increase the reference electricity-consumption rate e_0 = 1.85 kWh/km by 5% and 10%, respectively. These scenarios allow us to examine how increasing payload sensitivity affects route evaluation, energy consumption, estimated CO_2e emissions, and algorithmic behaviour.

For each vehicle k, the energy consumption is:

$$E_k = \sum_{i \epsilon V} \sum_{j \epsilon V} E_{ijk} \tag{10}$$

We define the total energy consumption of a complete routing solution as follows:

$$E_{total} = \sum_{k \epsilon K} E_k \tag{11}$$

CO_2 emission indicator

Although EVs produce no direct tailpipe emissions during route operation, their electricity consumption may induce indirect CO_2 emissions depending on the carbon intensity of the electricity mix used for charging. To support environmental interpretation, we define carbon indicator based on energy consumption as follows:

$$\mathrm{CO_2} = EF \times E_{total} \tag{12}$$

where: EF is used as a conversion factor to estimate CO_2 emissions from total energy consumption. In this study, EF = 0.718 kg CO_2e/kWh based on ADEME data for Morocco (Majaty et al., 2024; Ourya et al., 2023).

This quantity is not treated as a separate optimization objective. Instead, it is used as an environmental interpretation metric to evaluate routing performance. In this study, the linear formulation of CO_2 emissions was used to estimate indirect emissions associated with electricity consumption, it was adopted as an operational comparison indicator, not as a full life-cycle assessment in order to compare all routing alternatives under the same emission-factor assumption.

Fitness function and normalization

In the present study, a weighted fitness function was used to compare candidate routing solutions generated by the metaheuristics. Travelled distance and energy consumption were first normalized because they are measured in different units and cannot be directly aggregated in their raw form. The fitness function is defined as follows:

$$F = \omega_1 \frac{D_{total}}{D_{ref}} + \omega_2 \frac{E_{total}}{E_{ref}} + P \quad (13)$$

where:

$$D_{total} = \sum_{k\epsilon K} \sum_{i\epsilon V} \sum_{j\epsilon V, j\neq i} d_{ij} x_{ijk} \quad (14)$$

The reference values D_{ref} and E_{ref} were obtained from an initial greedy nearest-neighbour solution. This solution was used only for normalization purposes and was kept fixed for all algorithms and payload-sensitivity scenarios. D_{ref} corresponds to the total distance of this reference solution, while E_{ref} corresponds to its total energy consumption.

The parameters ω_1 and ω_2 are the distance and energy weights, respectively, with $\omega_1 + \omega_2 = 1$. The penalty term P is added only when a candidate solution violates operational constraints, mainly vehicle capacity or battery capacity. As all reported solutions satisfied these constraints, no penalty was applied in the final results. In the main experiments, a balanced weighting scheme was adopted, with $\omega_1 = 0.50$ and $\omega_2 = 0.50$, giving equal importance to distance and energy consumption. Two additional weighting schemes were then tested to examine the sensitivity of the results to the balanced weighting scheme. These configurations are defined as follows:

- Energy-oriented weighting scheme: $\omega_1 = 0.30$, $\omega_2 = 0.70$, which gives more weight to energy consumption.
- Distance-oriented weighting scheme: $\omega_1 = 0.70$, $\omega_2 = 0.30$, prioritizing travelled distance.

This composite formulation provides a unified eco-efficient fitness score that allows each routing solution to be assessed in terms of both operational efficiency and environmentally sensitive electricity use. However, total distance and total energy are also reported separately in the final analysis in order to preserve interpretability.

Routing problem constraints

The EVRP in SWM is subject to the following standard routing constraints:

Single service constraint

Each collection point must be visited exactly once by one EV:

$$\sum_{k\epsilon K} \sum_{i\epsilon V, i\neq j} x_{ijk} = 1, \forall j \in V - \{0\} \quad (15)$$

Flow conservation

For each visited node, the number of incoming arcs must equal the number of outgoing arcs:

$$\sum_{i\epsilon V, i\neq h} x_{ihk} - \sum_{j\epsilon V, j\neq h} x_{hjk} = 0, \quad \forall h \in V - \{0\}, \forall k \in K \quad (16)$$

Depot departure and return

Each EV route starts and ends at the depot:

$$\sum_{j\epsilon V, j\neq 0} x_{0jk} \leq 1, \quad \sum_{i\epsilon V, i\neq 0} x_{i0k} \leq 1, \forall k \in K \quad (17)$$

Payload capacity

The total collected waste assigned to vehicle k must not exceed its payload capacity:

$$\sum_{i\epsilon V, i\neq 0} q_i \times \sum_{j\epsilon V, j\neq i} x_{ijk} \leq Q, \forall k \in K \quad (18)$$

Battery capacity

The total route energy consumed by vehicle k should not exceed the available battery capacity of EV:

$$E_k \leq B, \forall k \in K \quad (19)$$

Solution encoding, route decoding, and feasibility checking

Before presenting the metaheuristic procedures, the common solution representation and route decoding mechanism are first introduced. In this work, GA, PSO, and SA all use the same permutation-based encoding and follow the same feasibility-checking rules. This ensures that the

three algorithms are evaluated under identical route construction conditions. First, each candidate solution is represented by a permutation of the waste collection points, excluding the depot from the encoded sequence:

$$S = (s_1, s_2, \ldots\ldots, s_n) \tag{20}$$

where: n is the number of waste collection points.

The depot is excluded from the permutation and is introduced only during the route-decoding stage. In this way, the permutation defines the visiting order of the collection points, while the final number of routes is determined dynamically during decoding, based on the vehicle capacity and battery-feasibility constraints. During decoding, the permutation is scanned from left to right and progressively split into feasible vehicle routes. Each route starts at the depot, and each collection point j is tested for insertion into the current route. Let i be the last visited node, l the onboard payload before travelling from i to j, and qj the waste demand at collection point j. Once j is served, the onboard payload becomes:

$$l' = l + q_j \tag{21}$$

Thus, the collection point j is accepted in the current route only if the following two feasibility conditions are satisfied:

First, the updated onboard payload satisfies the vehicle-capacity constraint:

$$l' \leq Q \tag{22}$$

Second, the vehicle can visit j and still return to the depot without exceeding the battery capacity:

$$E_{route} + E_{ij} + E_{j0} \leq B \tag{23}$$

where: E_{route} is the accumulated energy of the current route before inserting collection point j, E_{ij} denotes the energy required to travel from the last visited node i to j, E_{j0} is the energy required to return from collection point j to the depot after collecting its demand, B represents the battery capacity.

The arc energy terms are computed using the payload-sensitive energy formulation defined in the previous section. When both constraints are satisfied, collection point j is inserted into the current route. Otherwise, the current route is closed by returning to the depot, and a new route is started. After decoding, each solution is checked to ensure that all collection points are served exactly once, each route starts and ends at the depot, vehicle capacity is respected, and the energy consumed by each route does not exceed the battery capacity.

The same decoding and feasibility-checking procedure is applied to GA, PSO, and SA. Therefore, the three algorithms differ only in their search mechanisms within the permutation space, while route construction, payload sensitivity energy evaluation, and feasibility checking remain identical across all methods. The corresponding route-decoding and feasibility-checking procedure is summarized in Algorithm 1.

Input: collection point permutation S, vehicle capacity Q, battery capacity B, collection point demands q_j, distance matrix, e_0, and γ.

1. Initialize a new route starting from the depot.
2. Set current payload l=0 and current route energy E_{route}=0.
3. For each collection point j in S:
   a. identify the last node i in the current route;
   b. compute the updated payload $l'=l+q_j$;
   c. compute the energy required to travel from i to j;
   d. compute the energy required to return from j to the depot;
   e. if $l' \leq Q$ and $E_{route} + E_{ij} + E_{j0} \leq B$, insert j into the current route;
   f. otherwise, close the current route by returning to the depot and start a new route with j.
4. Close the last route by returning to the depot.
5. Recalculate route distance, route energy, route load, and feasibility indicators.

Output: decoded set of feasible vehicle routes.

Algorithm 1. Route decoding and feasibility checking

Metaheuristic algorithm resolution

In order to evaluate the proposed eco-efficient EVRP formulation, GA, PSO, and SA are applied under the same payload-sensitive routing framework, allowing a transparent comparison of their search behavior. These metaheuristics were selected because they represent complementary search optimization mechanisms, including evolutionary population search, probabilistic local improvement, and swarm learning intelligence. This choice is consistent with recent studies that have applied GA to green and EVs routing (Abid et al., 2024), PSO to sustainable MSW collection routing problems (Shen et al., 2023), and SA to waste collection and EVRP variants with local improvement mechanisms (Stamadianos et al., 2025). A brief description of each algorithm is provided below:

GA solution procedure

GA works by gradually improving several candidate routes; each candidate solution is represented as an ordered list of collection points. Initially, the population consisted of 28 individuals generated from the constructive reference sequence and several perturbed variants. Next, each chromosome was decoded into vehicle routes and evaluated using the same fitness function adopted for all algorithms. Parent selection was performed using the tournament selection mechanism; this is a very useful technique because good solutions are more able to reproduce while maintaining diversity. Then, GA applies recombination to create new solutions using an order-preserving crossover operator with a probability of 0.90. After recombination, mutation was applied with a probability of 0.35, meaning that 35% of the new individuals were modified. This technique is based on several operations, including swap, insertion, inversion, double insertion, and block relocation. To preserve high-quality solutions during the search and avoid losing a very good solution due to crossover or mutation operations, the three best individuals were saved by elitist replacement. The algorithm was run for 90 generations.

PSO solution procedure

PSO is inspired by the collective behavior of a group of solutions that learn together; it has been adapted to the discrete structure of the EVRP model, which is essentially a sequence of collection points problem. The swarm included 24 particles and was developed over 120 iterations; each particle is characterized by a personal and collective memory. Thus, the movement of the particles was effectively guided by the best individual and global solutions, using coefficients $c_1 = 0.55$ and $c_2 = 0.75$, respectively; their role is to control the influence of the two memories on the particles. Since classical velocity updates are not directly applicable to permutations, the update mechanism was adapted to sequence-based transformations. A perturbation probability of 0.25 was introduced to diversify the search and reduce premature stagnation. This perturbation allows for better tracking of good solutions while maintaining some exploration to discover other possible routes. Then, after each update, the resulting sequence was decoded and evaluated using the same fitness function adopted for the other algorithms.

In this study, PSO was implemented using a permutation-based representation adapted to the EVRP. In this representation, each particle corresponds to an ordered sequence of waste collection points, rather than a continuous position vector. As a result, the classical velocity update was replaced by a discrete swap-based update mechanism. At each iteration, swap sequences are generated to guide the current permutation toward the particle's personal best solution, p_{best}, and the global best solution, g_{best}. Swaps derived from p_{best} are applied with probability c_1=0.55, whereas swaps derived from g_{best} are applied with probability c_2=0.75. In addition, random permutation moves are introduced with probability 0.25 to maintain diversity in the swarm.

After each update, the permutation remains valid, since swap-based operations do not duplicate or remove collection points. The updated particle is then decoded into vehicle routes using the common route-decoding and feasibility-checking procedure also used for GA and SA. The personal best solution p_{best} and the global best solution g_{best} are updated whenever a better fitness value is found. In the experiments, PSO was run with 24 particles for 120 iterations.

In Algorithm 2, the symbol p represents the current particle permutation. The symbols p_{best} and g_{best} refer to the best permutation found by the particle itself and by the swarm, respectively. The terms $\Delta 1$ and $\Delta 2$ represent swap sequences, they are generated to move the current

permutation toward p_{best} and g_{best}. The coefficients c_1 and c_2 control the probability of applying swaps associated with p_{best} and g_{best}, while perturbation probability controls additional random permutation moves used for diversification. Once the update is completed, the new permutation is decoded into vehicle routes and evaluated using the common fitness function.

Input: swarm of particles, p_{best}, g_{best}, c_1, c_2, perturbation probability

Output: updated swarm and best solution

1. Initialize each particle as a valid permutation of waste collection points.
2. Evaluate each particle after route decoding.
3. Set the initial p_{best} of each particle and the initial g_{best} of the swarm.
4. For each iteration:
   - For each particle p:
     - Compute the swap sequence $\Delta 1$ between p and p_{best}.
     - Apply each swap in $\Delta 1$ with probability c_1.
     - Compute the swap sequence $\Delta 2$ between the updated particle and g_{best}.
     - Apply each swap in $\Delta 2$ with probability c_2.
     - With perturbation probability, apply random permutation moves for diversification.
     - Decode the updated permutation into feasible vehicle routes.
     - Evaluate distance, energy, estimated CO_2, penalty, and fitness.
     - If the new fitness improves the particle best, update p_{best}.
     - If the new fitness improves the global best, update g_{best}.
5. Return g_{best} as the best PSO solution.

Algorithm 2. Discrete PSO update mechanism

SA solution procedure

SA follows the principle of physical analogy of metal annealing, where the search process gradually moves from exploration to exploitation, becoming progressively more selective as the temperature decreases. In this study, SA was initialized first from a feasible construction sequence; this initialization gives SA a structured starting solution. After that, a local refinement procedure was applied to improve the initial solution before the main search phase. Candidate SA solutions were generated by neighborhood moves permutations including swap, insertion, inversion, double insertion, and block relocation. The initial temperature was fixed to $T_0 = 850$; this parameter is essential because it controls the level of exploration, meaning that when the temperature is high, SA is more able to accept a suboptimal solution, reducing the risk of premature convergence to local optima. The cooling rate was set at 0.9975, providing a gradual temperature decrease and maintaining exploration over several iterations. This algorithm was run for a maximum of 3000 iterations.

Case study and experimental design

Schneider benchmark dataset

The experimental study was conducted using the Schneider benchmark dataset (Schneider et al., 2014). Due to the limited availability of detailed real-world MSW collection data, this benchmark was selected because it represents one of the most widely used references in the EVRP literature and provides a standardized experimental framework for analyzing the effect of payload on energy consumption and CO_2 emissions on routing performance. The original customer nodes are treated as MSW collection points, while the depot remains the common distribution and return location. Customer demand values are considered to be the quantities of waste collected at each service point.

Baseline vs eco-efficient scenarios

In this work, two routing perspectives are examined. The first one is a baseline formulation where payload-impact coefficient γ=0, this means that energy consumption is proportional to travelled distance. In this scenario route quality is

evaluated only through total travel distance. The second scenario is an eco-efficient formulation where $\gamma > 0$, in which route evaluation combines travel distance and payload-sensitive energy consumption. This analysis allows us to show how the consideration of vehicle payload changes the assessment of routes in terms of energy consumption and CO_2 emissions.

Sensitivity analysis on γ

A sensitivity analysis was conducted on the payload impact coefficient γ, this analysis helps clarify how the transported payload affects energy consumption at the route level.

In this study, three main scenarios are considered:

- $\gamma = 0.00$: the distance is proportional to energy use;
- $\gamma = 0.05$: moderate payload-sensitive energy use;
- $\gamma = 0.10$: stronger payload-sensitive energy use.

These scenarios above are used to evaluate whether the relative performance of routing solutions and algorithms remains stable as the influence of vehicle payload on environmental indicators becomes stronger.

Evaluation metrics

The three algorithms are compared using both operational and environmental indicators, such as:

- total travel distance, expressed in km;
- total energy consumption in kWh;
- estimated CO_2 emissions in kg CO_2e;
- fitness value;
- computational runtime, expressed in seconds.

To account for stochastic variability, each algorithm was executed over 30 independent runs, and the reported results in tables below include mean values and standard deviations for algorithmic comparison, while best-run values are used only to provide best routing solution illustration.

RESULTS

Before the analysis of the algorithmic performance, all computational experiments were checked for structural feasibility. GA, PSO, and SA were executed over 30 independent runs, for each payload-sensitivity scenario (γ=0.00, 0.05, 0.10), under the same energy model, fitness function, route decoding procedure, and feasibility checking rules. For each run, travelled distance, energy consumption, estimated indirect CO_2e emissions, fitness value, runtime, and feasibility indicators were recorded. All reported final solutions were structurally feasible across the three algorithms and for all γ scenarios, confirming that all collection points were served, every route started and ended at the depot, and both vehicle capacity and battery constraints were respected.

The numerical analysis compares the performance of GA, PSO, and SA under the proposed payload-sensitive EVRP model. Table 2 summarizes the results obtained for the three payload-sensitivity scenarios, namely $\gamma = 0.00$, $\gamma = 0.05$, and $\gamma = 0.10$. This comparative analysis shows that the three metaheuristics produced feasible solutions within a relatively close performance range, particularly in terms of travelled distance, energy consumption, and estimated CO_2e

Table 2. Comparative performance of GA, PSO, and SA under different payload-sensitivity values over 30 independent runs

γ	Algorithm	Distance (km) Mean ± std	Energy (kWh) Mean ± std	CO_2e emissions (kg CO_2e) Mean ± std	Fitness Mean ± std	Runtime (s) Mean ± std
0.00	GA	1178.63±24.56	2180.47±45.43	1565.58±32.62	0.9391±0.020	4.85±0.74
0.00	PSO	1183.37±22.23	2189.24±41.13	1571.87±29.53	0.9429±0.018	5.64±0.96
0.00	SA	1183.51±21.57	2189.49±39.91	1572.05±28.66	0.9430±0.017	7.87±0.79
0.05	GA	1172.60±23.62	2209.92±45.15	1586.72±32.42	0.9430±0.019	4.75±0.74
0.05	PSO	1174.93±21.05	2214.33±39.74	1589.89±28.53	0.9449±0.017	5.65±0.88
0.05	SA	1177.76±20.87	2220.99±39.83	1594.67±28.59	0.9474±0.017	7.99±0.72
0.10	GA	1166.39±26.16	2238.86±50.22	1607.50±36.06	0.9467±0.021	4.74±0.73
0.10	PSO	1173.09±23.03	2250.89±44.39	1616.14±31.87	0.9519±0.019	5.44±0.80
0.10	SA	1177.95±19.00	2263.51±37.37	1625.20±26.83	0.9566±0.016	7.82±0.74

emissions. However, GA achieved the lowest mean values across the three γ scenarios.

The results show that increasing γ has a clear effect on energy consumption and estimated indirect CO_2e emissions, because a higher γ strengthens the contribution of vehicle payload to energy consumption. Across all algorithms, the average energy consumption increases between γ=0.00 and γ=0.10. As γ increases, all three algorithms show higher energy consumption. GA rises from 2180.47 to 2238.86 kWh, PSO from 2189.24 to 2250.89 kWh, and SA from 2189.49 to 2263.51 kWh. Estimated indirect CO_2e emissions follow the same pattern, by increasing from 1565.58 to 1607.50 kg CO_2e for GA, from 1571.87 to 1616.14 kg CO_2e for PSO, and from 1572.05 to 1625.20 kg CO_2e for SA. An important observation is that GA travels a shorter total distance as γ increases, decreasing from 1178.63 km at γ=0.00 to 1166.39 km at γ=0.10, but its energy consumption and emissions still rise. This result supports the idea that the evaluation route based on distance only is incomplete when vehicle payload affects energy use. Across the tested values of γ, GA provides the best performance, PSO remains close to GA, and SA delivers feasible but generally less competitive solutions.

Distribution of energy consumption and statistical reliability

The variability of total energy consumption over the 30 independent runs was examined using the boxplots in Figure 1 for the moderate payload-sensitivity scenario γ = 0.05. This analysis is important because the three algorithms GA, SA, and PSO are stochastic and they may produce different solutions across independent runs. These boxplots therefore help assess not only the average energy consumption, but also the stability and the variability of each method. The results show that GA, PSO, and SA produce solutions with relatively similar energy requirements under the moderate payload-sensitivity scenario γ= 0.05. GA has the lowest mean energy consumption, with 2209.92 kWh, followed closely by PSO with 2214.33 kWh. SA records the highest mean value, with 2220.99 kWh. As presented in the figure below, the overlap between the distributions shows that the algorithms perform within a close range at γ = 0.05. This justifies the use of non-parametric statistical tests to determine whether the observed descriptive differences are statistically meaningful.

In order to evaluate whether the observed algorithmic differences were statistically meaningful, the non-parametric Friedman test was applied to the 30 independent runs for each payload-sensitivity scenario. This test was useful because it helps to avoid relying only on descriptive mean values. Since the three metaheuristics are stochastic and their results vary across independent runs. It is especially relevant here in this study, because the algorithms show close performance for γ=0.00 and γ=0.05, meaning that small numerical differences should not be interpreted as strong algorithmic dominance without statistical support. For γ=0.00 and γ=0.05, no statistically significant differences were found among GA, PSO, and SA in terms of travelled distance, energy consumption, estimated indirect CO_2e emissions, or fitness. This suggests that, under the baseline and moderate payload-sensitivity settings, the

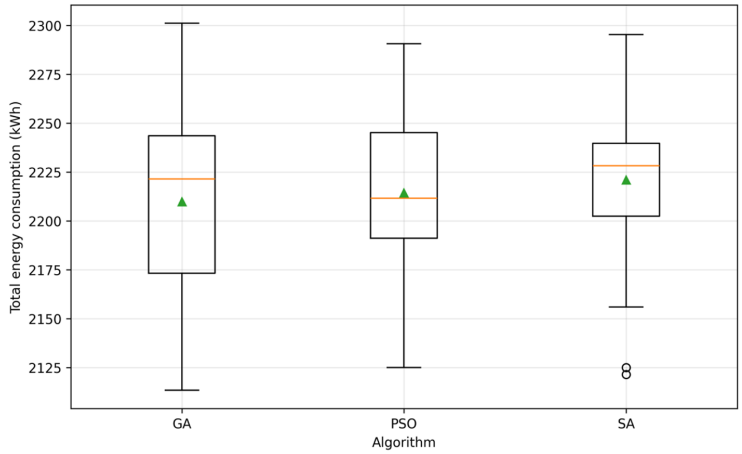

Figure 1. Distribution of total energy consumption obtained across independent runs at γ = 0.05. The orange line denotes the median and the green triangle indicates the mean value

differences observed between the algorithms remain mainly descriptive.

At γ=0.10, the Friedman test indicated statistically significant differences for the main solution-quality indicators, showing a clearer separation among the algorithms when the payload effect becomes stronger. As shown in Table 3, runtime differences were significant for all γ scenarios, which indicates that computational time varied consistently across the three methods. Overall, these results show that differences in runtime are systematic, whereas differences in solution quality become statistically evident only under the strongest payload-sensitivity scenario, γ=0.10.

Effect of the payload-sensitivity coefficient γ on energy consumption

To examine the effect of transported payload on route performance in the proposed EVRP framework, the payload-sensitivity coefficient γ was tested at three levels: 0.00, 0.05, and 0.10. This analysis helps to show how increasing the influence of transported payload changes the energy required by the same routing framework. Figure 2 complements the numerical results reported in Table 2, showing how mean energy consumption changes as γ increases. For the three algorithms GA, SA, and PSO, higher values of γ lead to higher electricity consumption, which confirms the importance of accounting for payload variation in electric MSW collection. The results show that GA demonstrates the smallest increase, its energy consumption rises from 2180.47 kWh at γ=0.00 to 2238.86 kWh at γ=0.10. Over the same interval, PSO increases from 2189.24 kWh to 2250.89 kWh, while SA reaches the highest value, with 2263.51 kWh at γ=0.10. These findings indicate that GA not only maintains the lowest mean energy values, but also shows the most limited increase when payload sensitivity becomes stronger. The results confirm that stronger payload sensitivity increases both energy consumption and estimated indirect CO_2e emissions, even when travelled distance remains stable or decreases slightly.

Distance–carbon trade-off analysis

The distance–carbon trade-off provides a clear interpretation of how payload-sensitive energy consumption γ affects route evaluation in the proposed EVRP model. Figure 3 shows that reducing the travel distance does not necessarily lead to lower CO_2 emissions when the payload effect is explicitly included in the energy model. This observation is particularly visible for the algorithm GA. As γ increases from 0.00 to 0.10, the mean travelled distance decreases from 1178.63 km to 1166.39 km. However, the estimated CO_2 emissions increase from 1565.58 kg CO_2e to 1607.50 kg CO_2e as presented in figure below. This means that the environmental performance of EVs in MSW collection route cannot be explained by distance only.

This result can be interpreted by considering the role of the collected waste payload along the route. In other words, when γ is higher, the model gives greater importance to the additional energy required to move the vehicle under changing payload conditions. Therefore, a route that is shorter in geometric terms may still become less favorable if it involves heavier payload movements or less efficient payload distribution. Similar behavior is observed for PSO and SA, whose estimated emissions also increase as γ rises. At γ = 0.10, GA still achieves the lowest mean emissions compared to the other algorithms, with 1607.50 kg CO_2e, compared with 1616.14 kg CO_2e for PSO and 1625.20 kg CO_2e for SA, indicating that GA remains more effective in balancing distance reduction with payload-sensitive energy performance. Thus, the trade-off analysis confirms the relevance of the proposed eco-efficient EVRP model. Route quality should not be assessed through route length only, especially in EVs for MSW collection where energy consumption depends on both movement and payload.

Table 3. Friedman test summary for algorithm comparison under each payload-sensitivity scenario

γ	Distance	Energy	CO_2e emissions	Fitness	Runtime
0.00	Not significant	Not significant	Not significant	Not significant	Significant
0.05	Not significant	Not significant	Not significant	Not significant	Significant
0.10	Significant	Significant	Significant	Significant	Significant

Note: Significance was assessed at α = 0.05 using the Friedman non-parametric test over 30 independent runs.

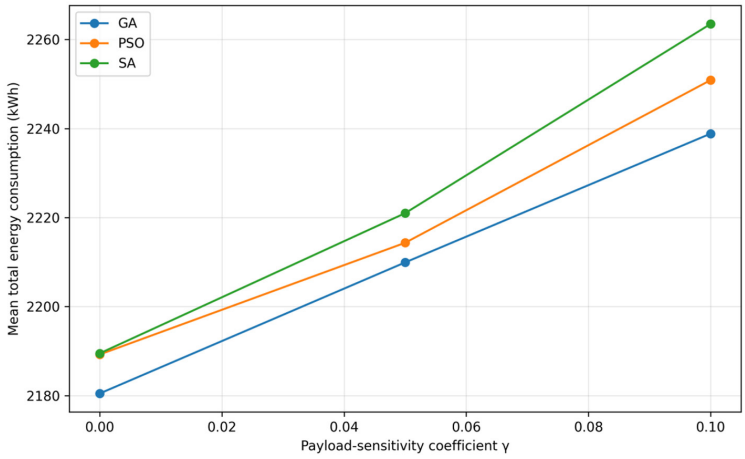

Figure 2. Sensitivity of energy consumption to the payload-sensitivity coefficient γ. Mean total energy consumption obtained by GA, PSO, and SA for the three payload-sensitivity levels γ = 0.00, 0.05, and 0.10.

Spatial analysis and load evolution of the best feasible solution at γ = 0.05

After the numerical comparison, the best feasible GA solution at γ=0.05 scenario was further examined from a spatial perspective in order to illustrate how the proposed eco-efficient EVRP model is organized on the network map. This step was useful because it links the quantitative results with the spatial organization of the collection service, showing how collection points are grouped and served from the depot. Figure 4 illustrates the corresponding routing plan produced by GA under the moderate payload-sensitivity at γ=0.05.

In this solution, as presented in the figure below, the 12 vehicles cover all waste collection points. The total travelled distance is 1121.9 km, while energy consumption and CO_2 emissions reach 2113.3 kWh and 1517.37 kg CO_2e, respectively. The associated fitness value is 0.902. Compared with the average GA performance in Table 2, this best run saves 50.7 km, 96.62 kWh, and 69.35 kg CO_2e. On the map, the routes appear organized into relatively clear service zones around the depot, rather than being dispersed across the entire network: routes close to the depot mainly serve nearby points in compact groups, whereas distant points are covered by longer routes reaching the periphery. This structure helps avoid unnecessary detours and supports the low energy and emission values obtained by GA. Therefore, this spatial pattern strengthens the numerical analysis by showing that the proposed eco-efficient EVRP model can produce a feasible and operationally significant waste collection plans.

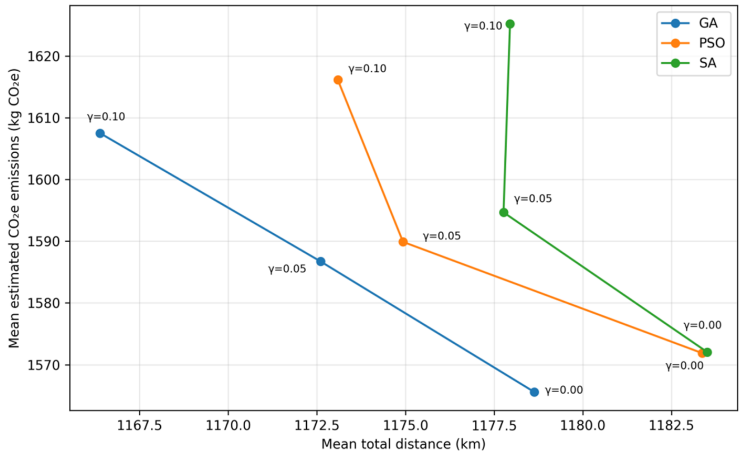

Figure 3. Distance–CO_2 emission trade-off across γ scenarios. Interaction between mean total distance and mean estimated CO_2 emissions for GA, PSO, and SA across the tested γ values

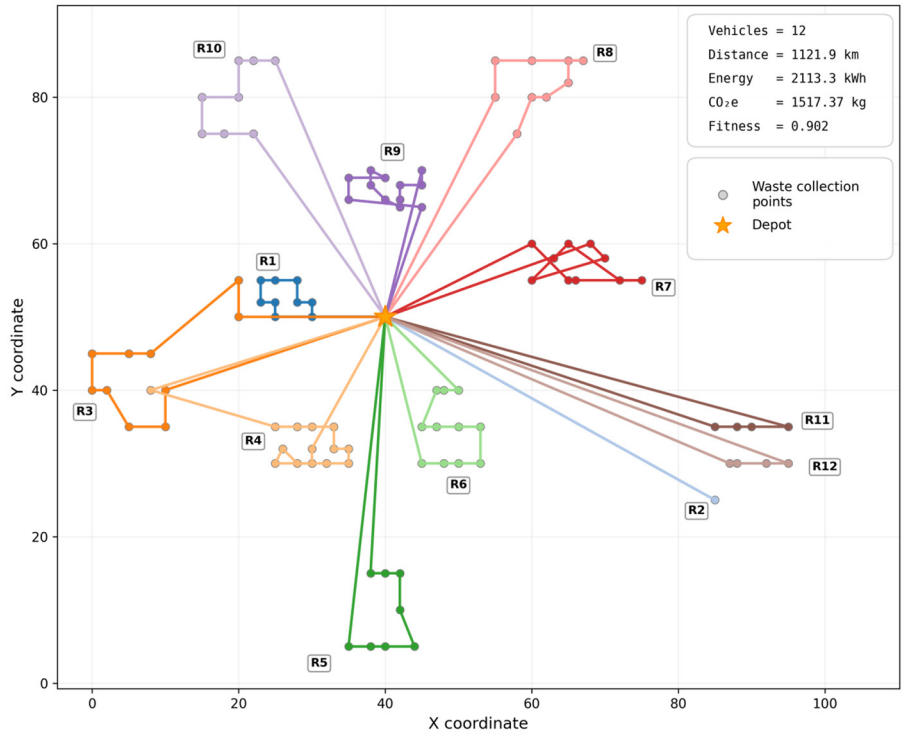

Figure 4. Best GA routing solution at $\gamma = 0.05$. Spatial representation of the best eco-efficient routing solution obtained by GA, showing the depot, waste collection points, vehicle routes, and main performance indicators

Figure 5 presents the evolution of vehicle load along the 12 routes obtained from the best feasible GA solution at $\gamma = 0.05$, presented in the previous figure. The dashed horizontal line represents the vehicle capacity. As expected in MSW collection, each route starts from the depot with an empty vehicle, and the load increases progressively as collection points are served.

The selected solution covers all 100 collection points through 12 feasible routes, with a total collected load of 1810 units. As shown in Figure 5, no route exceeds the vehicle capacity limit. Routes R4, R5, and R6 reach the full capacity of 200 units, while R8 and R10 end close to capacity with 190 units. Routes R3 and R9 reach 180 units, whereas R11 and R12 remain lighter, with 80 and 60 units, respectively. These lower loads are mainly associated with shorter or with service groups that are more spatially separated from the rest of the network.

The observed load profile shows that the decoder maintains route feasibility with respect to vehicle capacity, while reflecting the gradual accumulation of collected waste along each route. This also supports the logic of the payload-dependent energy model, where the energy required on a travelled arc is affected by both the arc distance and the payload carried by the vehicle during that movement.

Weight-sensitivity and robustness checks

In order to examine whether the main findings were influenced by the selected scalarization weights, a weight-sensitivity analysis was performed. In the fitness function, ω_1 denotes the weight assigned to the normalized travelled distance, whereas ω_2 denotes the weight assigned to the normalized energy consumption. Three weighting configurations were considered:

a) balanced setting, with $\omega_1 = 0.50$ and $\omega_2 = 0.50$,
b) distance-oriented setting, with $\omega_1 = 0.70$ and $\omega_2 = 0.30$,
c) energy-oriented setting with, $\omega_1 = 0.30$ and $\omega_2 = 0.70$.

Across the three weighting configurations, the energy model, emission factor, payload-sensitivity levels, algorithmic settings, and feasibility rules were kept constant. The comparison indicates that changing the balance between distance and energy in the fitness function does not meaningfully affect the main interpretation of the results. As presented in Table 4, all solutions remained structurally feasible, and only limited differences were observed in travelled distance, energy consumption, and estimated CO_2e emissions. These findings suggest that the conclusions are not dependent on one

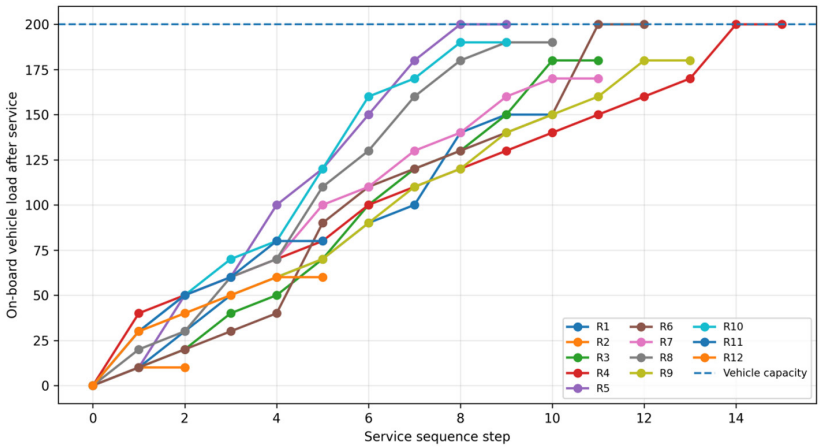

Figure 5. Load evolution of the 12 selected GA routes at $\gamma = 0.05$. The dashed line indicates the vehicle capacity of 200 units. All routes remain feasible, and no route exceeds the payload-capacity limit

arbitrary weighting scheme. Instead, the results are more strongly influenced by the payload-sensitivity coefficient γ than by the moderate variations applied to ω_1 and ω_2.

Computational problem-size diagnostic

In this study, a problem-size diagnostic was conducted to examine the behaviour of the proposed EVRP framework on sub-instances of the same Schneider benchmark-adapted network. The purpose of this analysis was to examine whether the implemented route decoding and feasibility checking procedure remains consistent when the number of collection points changes. Two reduced sub-instances were considered, N25 with 25 collection points and N50 with 50 collection points, and each case was evaluated for $\gamma = 0.00$, $\gamma = 0.05$, and $\gamma = 0.10$ over 30 independent runs. Table 5 reports aggregated diagnostic mean values across GA, PSO, and SA after computing the 30-run mean for each algorithm. Therefore, the table is used to summarize the global effect of problem size and payload sensitivity, rather than to rank the algorithms. All tested configurations remained structurally feasible, confirming that the decoding and feasibility checking procedure operated consistently across the reduced problem sizes.

The results confirm the effect of the payload sensitivity coefficient γ on environmental indicators. For N25, energy consumption increases from 429.96 kWh at $\gamma = 0.00$ to 441.70 kWh at $\gamma = 0.10$, while estimated CO_2e emissions increase from 308.71 to 317.14 kg CO_2e. During the same interval, travelled distance slightly decreases from 232.41 to 229.58 km. A similar behaviour is observed for N50, where distance decreases from 457.27 to 454.13 km, whereas energy consumption rises from 845.96 to 877.25 kWh and CO_2e emissions increase from 607.40 to 629.86 kg CO_2e. These results reinforce the main finding of the study: travelled distance alone is not sufficient to evaluate electric MSW collection routes. Even when distance remains stable or slightly decreases, a stronger payload-sensitivity effect increases energy consumption and estimated CO_2e emissions. This confirms the importance of incorporating payload-dependent energy consumption

Table 4. Weight-sensitivity robustness check at $\gamma = 0.10$ over 30 independent runs

Weighting scenario	ω_1 Distance	ω_2 Energy	Best Algorithm	Distance (km)	Energy (kWh)	CO_2e emissions (kg CO_2e)	Runtime (s)
Distance-oriented	0.70	0.30	GA	1164.48	2235.30	1604.95	6.38
Balanced	0.50	0.5	GA	1166.39	2238.86	1607.50	4.74
Energy-oriented	0.30	0.7	GA	1166.77	2239.57	1608.01	5.75

Note: The table reports the mean values best-performing algorithm under the strongest payload-sensitivity scenario, $\gamma = 0.10$. Fitness values are not directly compared across weighting schemes because the fitness definition changes when ω_1 and ω_2 are modified.

Table 5. Problem-size and payload-sensitivity diagnostic on reduced sub-instances

Size	γ	Distance (km)	Energy (kWh)	CO_2e emissions (kg CO_2e)	Runtime (s)
N25	0.00	232.41	429.96	308.71	2.67
N25	0.05	230.27	434.60	312.04	2.55
N25	0.10	229.58	441.70	317.14	2.60
N50	0.00	457.27	845.96	607.40	3.45
N50	0.05	454.43	859.34	617.01	3.44
N50	0.10	454.13	877.25	629.86	3.48

Note: Values are aggregated diagnostic means across GA, PSO, and SA after computing 30-run means for each algorithm. They are not best-run values and are used only to summarize the effect of problem size and γ.

into the EVRP evaluation. However, this analysis should be interpreted as a controlled problem-size diagnostic rather than as a general proof of large-scale scalability.

CONCLUSIONS

This study demonstrates that the environmental assessment of EVRP solutions for MSW collection is sensitive to the representation of vehicle payload within the energy-consumption model. The results reveal a consistent distance–energy–emission trade-off, where reductions in travelled distance do not necessarily lead to lower energy consumption or CO_2 emissions when payload effects are explicitly considered. This finding establishes the payload-sensitivity coefficient γ as a key factor influencing the environmental evaluation of routing solutions. Furthermore, the comparative analysis shows that algorithmic performance is not invariant to payload-dependent energy modelling, as the relative performance patterns of GA, PSO, and SA become more clearly differentiated with increasing payload sensitivity. Therefore, the main contribution of this work is the demonstration that incorporating payload-dependent energy consumption provides additional discriminatory power for evaluating EVRP solutions and exposes environmental differences that remain hidden under conventional distance-based routing formulations.

REFERENCES

1. Abdel-Shafy, H.I., Mansour, M.S.M. (2018). Solid waste issue: Sources, composition, disposal, recycling, and valorization. *Egyptian Journal of Petroleum, 27*(4), 1275–1290. https://doi.org/10.1016/j.ejpe.2018.07.003
2. Abid, M., Tabaa, M., Hachimi, H. (2024). Electric vehicle routing problem with an enhanced vehicle dispatching approach considering real-life data. *Energies*, *17*(7), 1596. https://doi.org/10.3390/en17071596
3. Ali, M., Marvuglia, A., Geng, Y., Chaudhry, N., Khokhar, S. (2018). Emergy based carbon footprinting of household solid waste management scenarios in Pakistan. *Resources, Conservation and Recycling*, *131*, 283–296. https://doi.org/10.1016/j.resconrec.2017.10.011
4. Amine Masmoudi, M., Coelho, L.C., Demir, E. (2022). Plug-in hybrid electric refuse vehicle routing problem for waste collection. *Transportation Research Part E: Logistics and Transportation Review*, *166*, 102875. https://doi.org/10.1016/j.tre.2022.102875
5. Bányai, T., Tamás, P., Illés, B., Stankevičiūtė, Ž., Bányai, Á. (2019). Optimization of municipal waste collection routing: Impact of Industry 4.0 technologies on environmental awareness and sustainability. *International Journal of Environmental Research and Public Health*, *16*(4), 634. https://doi.org/10.3390/ijerph16040634
6. Bouleft, Y., Elhilali Alaoui, A. (2023). Dynamic multi-compartment vehicle routing problem for smart waste collection. *Applied System Innovation*, *6*(1), 30. https://doi.org/10.3390/asi6010030
7. Carlos, M., Gallardo, A., Edo-Alcón, N., Abaso, J.R. (2019). Influence of the municipal solid waste collection system on the time spent at a collection point: A case study. *Sustainability*, *11*(22), 6481. https://doi.org/10.3390/su11226481
8. Das, S., Baral, A., Rafizul, I.M., Berner, S. (2024). Efficiency enhancement in waste management through GIS-based route optimization. *Cleaner Engineering and Technology*, *21*, 100775. https://doi.org/10.1016/j.clet.2024.100775
9. Dotoli, M., Epicoco, N. (2017). A vehicle routing technique for hazardous waste collection. *IFAC-PapersOnLine*, *50*(1), 9694–9699. https://doi.org/10.1016/j.ifacol.2017.08.2051

10. Erdem, M. (2022). Optimisation of sustainable urban recycling waste collection and routing with heterogeneous electric vehicles. *Sustainable Cities and Society*, *80*, 103785. https://doi.org/10.1016/j.scs.2022.103785
11. Fan, L., Liu, C., Dai, B., Li, J., Wu, Z., Guo, Y. (2023). Electric vehicle routing problem considering energy differences of charging stations. *Journal of Cleaner Production*, *418*, 138184. https://doi.org/10.1016/j.jclepro.2023.138184
12. Li, T., Deng, S., Lu, C., Wang, Y., Liao, H. (2023). Optimization of green vehicle paths considering the impact of carbon emissions: A case study of municipal solid waste collection and transportation. *Sustainability*, *15*(22), 16128. https://doi.org/10.3390/su152216128
13. Lin, K., Musa, S.N., Lee, H.Y., Yap, H.J. (2024). Sustainable location-routing problem for medical waste management using electric vehicles. *Sustainable Cities and Society*, *112*, 105598. https://doi.org/10.1016/j.scs.2024.105598
14. Liu, Z., Sun, L., Zuo, X., Li, H. (2024). Heterogeneous electric vehicle routing problem with multiple compartments and multiple trips for the collection of classified waste. *International Journal of Crowd Science*, *8*(3), 130–139. https://doi.org/10.26599/IJCS.2023.9100030
15. Majaty, S.E., Touzani, A., Kasseh, Y. (2024). Circular economy as an important lever to reduce greenhouse gas emissions: Case of an electricity distribution company in Morocco. *Nature Environment and Pollution Technology*, *23*(2), 819–828. https://doi.org/10.46488/NEPT.2024.v23i02.018
16. Mohammadi, M., Rahmanifar, G., Hajiaghaei-Keshteli, M., Fusco, G., Colombaroni, C., Sherafat, A. (2023). A dynamic approach for the multi-compartment vehicle routing problem in waste management. *Renewable and Sustainable Energy Reviews*, *184*, 113526. https://doi.org/10.1016/j.rser.2023.113526
17. Mojtahedi, M., Fathollahi-Fard, A.M., Tavakkoli-Moghaddam, R., Newton, S. (2021). Sustainable vehicle routing problem for coordinated solid waste management. *Journal of Industrial Information Integration*, *23*, 100220. https://doi.org/10.1016/j.jii.2021.100220
18. Ourya, I., Nabil, N., Abderafi, S., Boutammachte, N., Rachidi, S. (2023). Assessment of green hydrogen production in Morocco, using hybrid renewable sources (PV and wind). *International Journal of Hydrogen Energy*, *48*(96), 37428–37442. https://doi.org/10.1016/j.ijhydene.2022.12.362
19. Pujara, Y., Pathak, P., Sharma, A., Govani, J. (2019). Review on Indian municipal solid waste management practices for reduction of environmental impacts to achieve sustainable development goals. *Journal of Environmental Management*, *248*, 109238. https://doi.org/10.1016/j.jenvman.2019.07.009
20. Rahmanifar, G., Mohammadi, M., Sherafat, A., Hajiaghaei-Keshteli, M., Fusco, G., Colombaroni, C. (2023). Heuristic approaches to address vehicle routing problem in the Iot-based waste management system. *Expert Systems with Applications*, *220*, 119708. https://doi.org/10.1016/j.eswa.2023.119708
21. Rathore, P., Sarmah, S.P. (2019). Modeling transfer station locations considering source separation of solid waste in urban centers: A case study of Bilaspur city, India. *Journal of Cleaner Production*, *211*, 44–60. https://doi.org/10.1016/j.jclepro.2018.11.100
22. Roberts, K.P., Turner, D.A., Coello, J., Stringfellow, A.M., Bello, I.A., Powrie, W., Watson, G.V.R. (2018). SWIMS: A dynamic life cycle-based optimisation and decision support tool for solid waste management. *Journal of Cleaner Production*, *196*, 547–563. https://doi.org/10.1016/j.jclepro.2018.05.265
23. Sarmah, S.P., Yadav, R., Rathore, P. (2019). Development of vehicle routing model in urban solid waste management system under periodic variation: A case study. *IFAC-PapersOnLine*, *52*(13), 1961–1965. https://doi.org/10.1016/j.ifacol.2019.11.490
24. Schmid, F., Taube, L., Rieck, J., Behrendt, F. (2021). Electrification of waste collection vehicles: Technoeconomic analysis based on an energy demand simulation using real-life operational data. *IEEE Transactions on Transportation Electrification*, *7*(2), 604–615. https://doi.org/10.1109/TTE.2020.3031072
25. Schneider, M., Stenger, A., Goeke, D. (2014). The electric vehicle-routing problem with time windows and recharging stations. *Transportation Science*, *48*(4), 500–520. https://doi.org/10.1287/trsc.2013.0490
26. Shen, X., Pan, H., Ge, Z., Chen, W., Song, L., Wang, S. (2023). Energy-efficient multi-trip routing for municipal solid waste collection by contribution-based adaptive particle swarm optimization. *Complex System Modeling and Simulation*, *3*(3), 202–219. https://doi.org/10.23919/CSMS.2023.0008
27. Silva, A.S., Alves, F., Diaz De Tuesta, J.L., Rocha, A.M.A.C., Pereira, A.I., Silva, A.M.T., Gomes, H.T. (2023). Capacitated waste collection problem solution using an open-source tool. *Computers*, *12*(1), 15. https://doi.org/10.3390/computers12010015
28. Stamadianos, T., Kyriakakis, N.A., Marinaki, M., Marinakis, Y. (2025). A hybrid simulated annealing and variable neighborhood search algorithm for the close-open electric vehicle routing problem. *Annals of Mathematics and Artificial Intelligence*, *93*, 817–840. https://doi.org/10.1007/s10472-023-09858-x
29. Wang, Y., Zhou, J., Sun, Y., Fan, J., Wang, Z., Wang, H. (2023). Collaborative multidepot electric vehicle routing problem with time windows and shared charging stations. *Expert Systems with*

Applications, *219*, 119654. https://doi.org/10.1016/j.eswa.2023.119654

30. Wang, Y., Zhou, J., Sun, Y., Wang, X., Zhe, J., Wang, H. (2022). Electric vehicle charging station location-routing problem with time windows and resource sharing. *Sustainability*, *14*(18), 11681. https://doi.org/10.3390/su141811681
31. Yadav, V., Karmakar, S. (2020). Sustainable collection and transportation of municipal solid waste in urban centers. *Sustainable Cities and Society*, *53*, 101937. https://doi.org/10.1016/j.scs.2019.101937
32. Yang, J., Tao, F., Zhong, Y. (2022). Dynamic routing for waste collection and transportation with multi-compartment electric vehicle using smart waste bins. *Waste Management & Research: The Journal for a Sustainable Circular Economy*, *40*(8), 1199–1211. https://doi.org/10.1177/0734242X211069738
33. Zamanian, A., Khodaei, Z., Ziarati, K. (2024). Municipal solid waste management using electric vehicle by variable neighbourhood search algorithm. *International Journal of Systems Science: Operations & Logistics*, *11*(1), 2393859. https://doi.org/10.1080/23302674.2024.2393859
34. Zhang, S., Zhou, T., Fang, C., Yang, S. (2024). A novel collaborative electric vehicle routing problem with multiple prioritized time windows and time-dependent hybrid recharging. *Expert Systems with Applications*, *244*, 122990. https://doi.org/10.1016/j.eswa.2023.122990